Proceedings Paper:
Ghaffarlouy Raef, Ali, Marvin, Andy, BALE, SIMON JONATHAN et al. (2025) Shielding Effectiveness of Enclosures: Characterising the Transition from Reverberant to Resonant Behavior. In: IEEE International Symposium on Electromagnetic Compatibility - EMC Europe 2025:proceedings. IEEE International Symposium on Electromagnetic Compatibility, 01-05 Sep 2025 EMC Europe. IEEE, FRA.

https://doi.org/10.1109/EMCEurope61644.2025.11176219

Shielding Effectiveness of Enclosures: Characterising the Transition from Reverberant to Resonant Behavior

Ali Ghaffarlouy Raef, Andrew C. Marvin, Simon J. Bale, Martin P. Robinson, John F. Dawson

School of Physics, Engineering, and Technology, University of York, UK
{ali.raef, andy.marvin, simon.bale, martin.robinson, john.dawson}@york.ac.uk

***Abstract* — Understanding the shielding effectiveness (SE) of enclosures across different frequency ranges is crucial for electromagnetic compatibility (EMC) applications. While well-established methods exist for evaluating SE in the reverberant frequency range, the transition between reverberant and resonant behavior remains less explored. This paper investigates the shielding performance of a brass enclosure containing Transmission Line Representative Contents (TL ReCos) across the reverberant, transition, and resonant frequency regions. The study employs a mechanically stirred reverberation chamber (RC) to analyze the SE response using a combination of wall-mounted and internal monopole antennas. Results confirm the existence of a transition frequency region with change in field distribution and SE behavior. The findings highlight how variations in frequency, internal contents, and measurement positions influence SE, providing valuable insights for enclosure design and EMC testing.**

***Keywords* — Shielding effectiveness, reverberation chamber, transition frequency region, electromagnetic compatibility, shielding enclosures, power balance method.**

I. Introduction

The presence of electronic systems and devices in electromagnetic (EM) environments poses significant challenges. These environments can cause damage or degradation in the performance of such systems. EM interference can arise from various sources, ranging from natural atmospheric phenomena, un-intentional, and intentional interference generated by manufactured devices. To mitigate these interferences, shielding enclosures with different types of materials are employed to house sensitive electronic devices [1], [2].

In recent years, the increasing demand for shielding enclosures of various sizes and types for electromagnetic interference (EMI) mitigation has increased the importance of evaluating their shielding effectiveness (SE) under different conditions and with varying internal contents [3].

IEEE Std 299.1 [4] discusses the use of the reverberation chamber (RC) method to evaluate the behavior of small enclosures with linear dimensions between 0.1m and 2m that are electrically large enough to be considered reverberant. For reverberant enclosures of this size, well-established methods are available to assess their SE [1], [5], [6].

This project has received funding from the European Union's EU Framework Programme for Research and Innovation Europe Horizon under Grant Agreement No 101072881.

However, as the frequency decreases (and the wavelength increases), these enclosures become electrically smaller. Consequently, the uniform power density characteristic of the reverberant frequency range transitions to a non-uniform distribution in the lower non-reverberant frequency range. In this paper, we discuss the transition frequency range between the reverberant frequency range and the resonant frequency range (Fig. 1). The transition from the reverberant to the resonant frequency range is significant, as the field strength and distribution within the enclosure and hence the SE begin to vary depending on the position, frequency, and placement of internal contents.

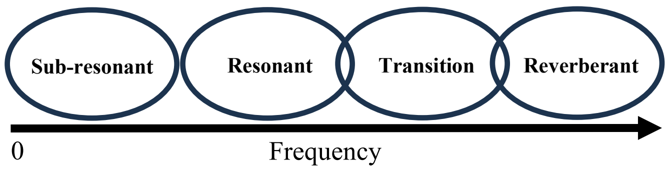

Fig. 1. The transition frequency range placement and merging with resonant and reverberant frequency ranges.

It is important to note that while we define these three frequency regions (reverberant, transition, and resonant), the boundaries between them are not distinct. Instead, each region gradually merges into the next as the frequency changes (Fig. 1). Moreover, the boundary between the sub-resonant and resonant regions is defined by the first resonance of the enclosure. In the resonant frequency range, discrete resonant modes determine the measured SE, resulting in rapid variations with frequency, including low or even negative SE values expressed in dB, and minimal or no frequency overlap [7].

In [1], an improved technique for predicting the SE of electrically large enclosures (reverberant enclosures) with various apertures and contents by incorporating the power balance method (PWB) is presented. In this paper, the enclosure's behavior as it transitions from the reverberant to the resonant frequency range is described and the results confirm the existence of a transition frequency region.

Section II provides detailed descriptions of the representative contents used in this study within the enclosure, the monopole probes employed for measurements, and the positions of these probes within the enclosure. Discussion of the measurement setup is provided in section III. The results are analyzed and discussed in Section IV. Conclusions are presented in Section V.

II. Instrumented Contents

Shielded enclosures are never used in isolation and any enclosure will be deployed with internal contents comprising circuit boards and other components. The evaluation of SE for enclosures populated with contents is thus more useful than for empty enclosures as any contents absorb electromagnetic energy, change the field distribution and result in a different SE to that of the empty enclosure. To represent the contents (i.e. printed circuit boards (PCBs)) typically housed in such enclosures, Transmission Line Representative Contents (TL ReCos) were employed. These have been described in [1] and [8]. These basic TL ReCo units consist of sixteen unit-cells, each containing twenty-nine resistively loaded transmission line tracks. The unit cells are evenly distributed, with eight cells mounted on each side of a double-sided carrier PCB. Each basic TL ReCo has dimensions of 280mm × 145mm. These are illustrated in Fig. 2 and Fig. 3. The TL ReCos mimic the absorptive behavior of real circuit boards in a controlled and repeatable way.

In this work, five stacked TL ReCos (four basic and one with antennas, spaced 80mm apart, see below) were utilized as the contents, alongside three 20mm monopole antennas (monopoles 1-3 described in [1]) mounted on orthogonal walls of the enclosure (Fig. 2). The end TL ReCo, positioned adjacent to the empty portion of the enclosure's volume, was equipped with four additional monopole antennas. Fig. 3 shows these antennas (monopoles A-D) which were positioned on one side of the Antenna TL ReCo and connected through the back wall of the enclosure via coaxial cables. This configuration enabled measurements at the same positions within the enclosure as described in [1], along with field measurements at positions on the absorbing surface of the Antenna TL ReCo. During the measurement, the Antenna TL ReCo was rotated to place its antennas on either side including in the gap between the ReCos (Fig. 2). During all measurements, all antennas were terminated with 50Ω loads to ensure consistent results.

III. Measurement Approach

A. Test Enclosure and RC

In this study, the measurements were performed with the brass enclosure described in [1], that has the dimensions of 600mm × 500mm × 300mm as shown in Fig. 4 within a mechanically stirred RC following the procedure described in [4]. The enclosure has a rectangular aperture measuring 140mm × 40mm on one of the 600mm × 300mm faces.

The RC located in the University of York laboratory has dimensions of 4.7m × 3.0m × 2.37m, with its fundamental TE_{110} mode at 59MHz. It is highly over-moded above 300MHz, which is the frequency range of interest for this study. A mechanical stirrer with one hundred positions per full rotation was employed to achieve mode stirring within the RC. A Vector Network Analyzer (VNA) with an intermediate frequency bandwidth (IFBW) of 10kHz and output power level of 10dBm was used to measure the S-parameters between the transmit (Tx) antenna in the RC and each one of the receive (Rx) antennas for reference and shielding measurements involving the enclosure.

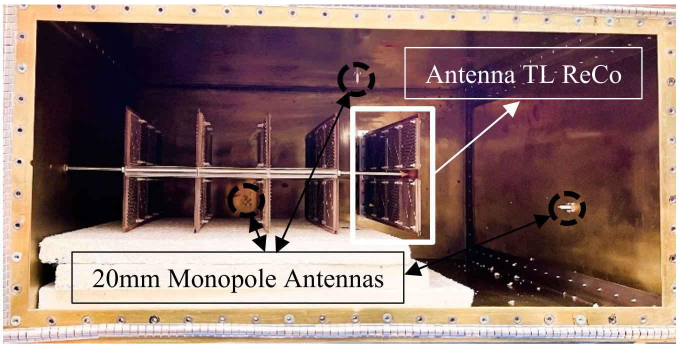

Fig. 2. The placement of the Antenna TL ReCo, other basic TL ReCos, and monopole antennas within the enclosure volume (the enclosure face with the aperture dimension 140mm × 40mm removed to show internal contents).

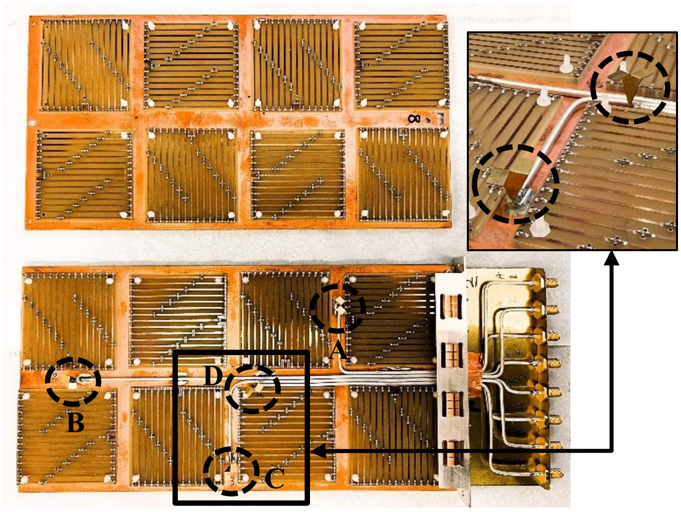

Fig. 3. The Antenna TL ReCo with four monopole antennas in random positions (bottom). Basic TL ReCo (dimensions 280mm × 145mm) as a surrogate for PCB (top) [8].

Fig. 4. University of York RC showing the enclosure with its 140mm × 40mm aperture.

The dimensions of the brass enclosure are limited and placing a mode stirrer inside the enclosure was not feasible. For this reason, for higher frequency measurements (see Section B), both mechanical stirrer and frequency stirring were implemented, whereas for lower frequencies (see Section III.C), results were averaged only over stirrer positions.

To investigate the behavior of the enclosure across the reverberant, transition, and resonant frequency regions, particularly considering the discrete resonances and the Q-bandwidth of resonant modes at lower frequencies, measurements were conducted in two parts to achieve better resolution at lower frequencies. The first part covered the frequency range of 2GHz to 20GHz with 10,001 frequency points (1.8MHz frequency step), while the second part spanned from 300MHz to 2.3GHz with 20,001 frequency points (100kHz frequency step) to capture all the resonant mode responses comprehensively.

For the unshielded reference measurements, as illustrated in Fig. 5, all monopoles were positioned within the RC without the enclosure and measured separately for each frequency range.

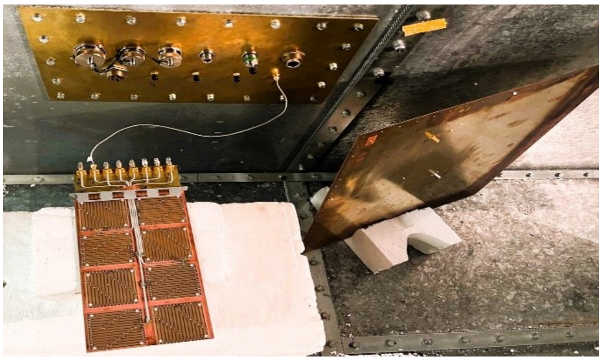

Fig. 5. The unshielded reference measurement of monopoles inside the RC.

B. 2GHz to 20GHz

In [1], the shielding behavior of the brass enclosure with a rectangular aperture and the inclusion of basic TL ReCos was discussed. The SE results were averaged across the three monopole antennas, mechanical stirrer positions, and over a specified frequency range. To further evaluate the SE definition in the reverberant frequency range and verify the reliability of the results, new measurements were performed using the new set of monopole antennas mounted on the Antenna TL ReCo.

As illustrated in Fig. 6, the averaged SE results, which are averaged over hundred frequency points (180MHz), obtained from the four antennas on the Antenna TL ReCo align well with the results from the earlier study, which utilized the three wall mounted monopole antennas. These findings confirm that within the reverberant frequency range, the enclosure exhibits consistent average shielding performance across different antenna positions within its volume.

However, as the frequency decreases, average SE behavior becomes increasingly influenced by the positions of the antennas, leading to greater variability. This trend is evident in Fig. 6, where at approximately 4GHz, the difference between the two averaged SE results is about 1dB. As the frequency decreases to 2GHz, this difference grows to approximately 3dB, highlighting the stronger dependence of SE behavior on antenna placement as frequency decreases.

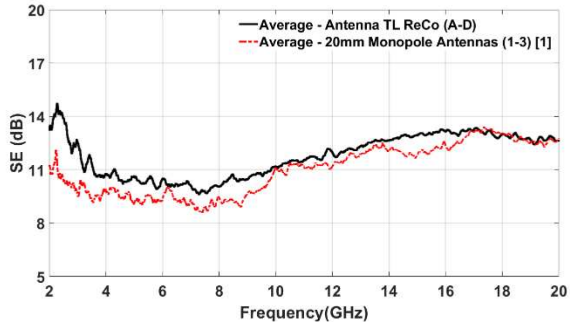

Fig. 6. Comparison of new average SE results (Antenna TL ReCo monopoles) with average SE results of 20mm monopole antennas in [1].

C. 300MHz to 2.3GHz

For the dimensions of the experimental brass enclosure, the fundamental TE_{110} resonance for the empty enclosure occurs at 390MHz. Whilst this minimum resonant frequency, derived from the well-known Helmholtz equation offers a guide to the extent of the resonant frequency range, the presence of the ReCos and their supporting rods, visible in Fig. 2, perturbs the Helmholtz resonant frequencies and potentially adds further resonances.

Within the frequency range below where the enclosure begins to exhibit reverberant behavior, several challenges arise. First, in this range, the field distribution is highly non-uniform due to the excitation of discrete resonances, making it sensitive to the position and polarization of the antennas. Second, the sharp discrete resonances contribute to greater variability in SE results. Additionally, the detailed configuration of the enclosure, including the volume, the position of its contents, and the placement of apertures on its walls, also significantly influences the shielding behavior.

D. SE Definition

The SE definition for the non-reverberant frequency range provided in [3], [4] is voltage-based, where SE is defined as the ratio of the induced voltage of an antenna over a ground plane inside the RC to the induced voltage of the same antenna inside the enclosure.

However, for consistency across the whole frequency range, this study utilizes the RC method to measure the shielding behavior of the enclosure, applying the power-based definition to calculate SE. In this approach, SE is determined as the ratio of the average power density outside the enclosure to the average power density inside the enclosure [4]:

$$SE = \frac{\langle |S_{21,REF}|^2 \rangle}{\langle |S_{21,ENC}|^2 \rangle}$$

here, $S_{21,REF}$ is coupling between the Tx antenna in the RC and each one of the reference Rx antennas placed outside the enclosure, and $S_{21,ENC}$ is the coupling between the Tx antenna in the RC and each one of the antennas placed inside the enclosure. Moreover, ⟨...⟩ denotes the averaging over all mechanical stirrer positions.

IV. Results and Discussion

Figures 7 to 9 present the averaged SE results for all the antenna probes within the enclosure. These results are averaged solely over the mechanical stirrer positions. To provide greater clarity, the frequency range in each figure is divided into three subranges (a, b, and c) which approximately correspond to the resonant, transition, and reverberant regions.

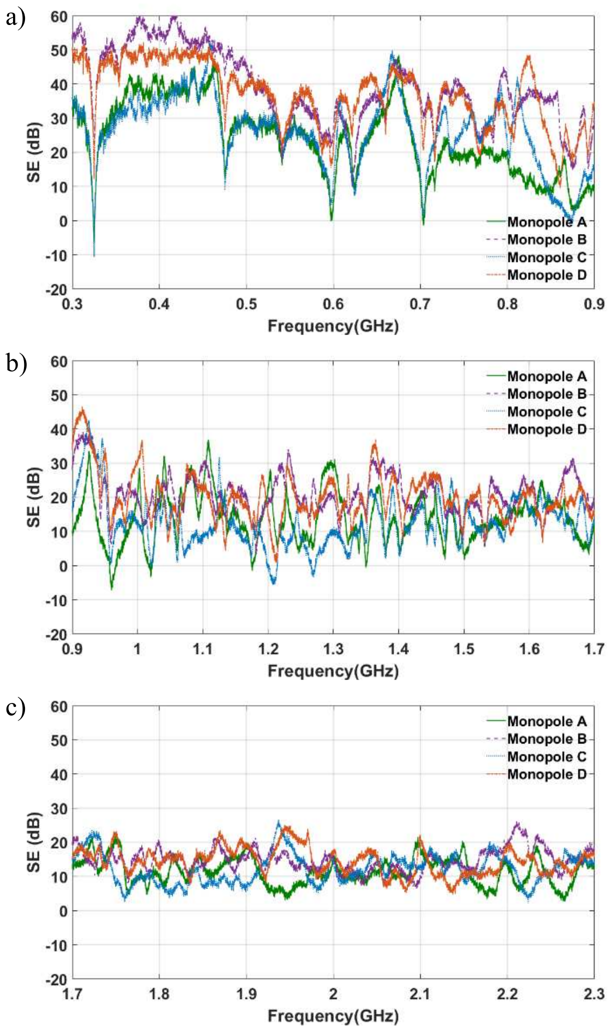

Fig. 7. Averaged SE calculated using the monopole antennas on the Antenna TL ReCo, a) resonant region, b) transition region, and c) reverberant region.

Figure 7 illustrates the averaged SE results of the monopoles mounted on the Antenna TL ReCo. In Fig. 7a, corresponding to the resonant frequency range, distinct resonances are observed. The averaged SE values vary significantly, with some negative values as low as -10dB at 325MHz and 0dB at 595MHz, indicating critical vulnerabilities in shielding performance. Additionally, while the fundamental resonance of the empty enclosure occurs at 390MHz, the presence of contents within the enclosure causes a shift in this resonance to 325MHz, demonstrating that the internal field configuration changes in the presence of populated enclosures.

In Fig. 7b, which covers the transition frequency range, the averaged SE behavior becomes less variable compared to the resonant range. Although substantial variations in averaged SE values are still present, the extent of these variations is reduced, resulting in smaller differences between SE maxima and minima.

In Fig. 7c, representing the start of the reverberant frequency range, the averaged SE fluctuations and variations further decrease. This results in more uniform shielding behavior and a smaller distribution of SE values at higher frequencies. It is also evident that, although monopoles C and D on the Antenna TL ReCo are physically closer to each other than the other two monopoles (Fig. 3), they still exhibit significantly different averaged SE values in the resonant and transition ranges. As the frequency increases into the reverberant range, their averaged SE values converge, demonstrating similar behavior. This highlights the impact of both position and frequency on SE variability in different frequency regions.

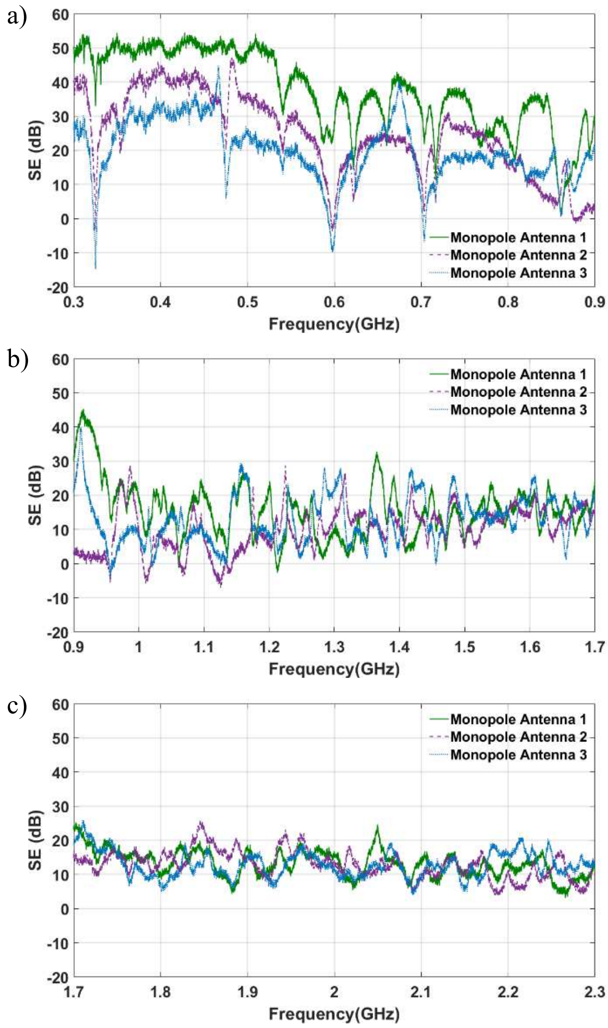

Fig. 8. Averaged SE calculated using the 20mm monopole antennas mounted on the walls of the enclosure, a) resonant region, b) transition region, and c) reverberant region.

In Fig. 8, the averaged SE results for the 20mm monopole antennas mounted on the enclosure walls are presented. The plots highlight clear distinctions between the results from different antennas, particularly in the resonant and transition frequency regions due to the antenna placement within the enclosure.

At lower frequencies, monopole antenna 1 consistently demonstrates higher averaged SE values, while monopole antenna 3 shows lower averaged SE values. This behavior reflects the sensitivity of averaged SE to antenna placement in the resonant region with each monopole capturing a different set of resonant averaged SE minima. Additionally, since the monopoles are mounted on three orthogonal walls, the averaged SE results show greater variability compared to the monopoles on the Antenna TL ReCo. As the frequency increases into the reverberant range, the averaged SE results from all antennas converge to approximately 15dB. This convergence indicates a reduction in variability due to increased coupling and mode overlap, a characteristic of reverberant behavior.

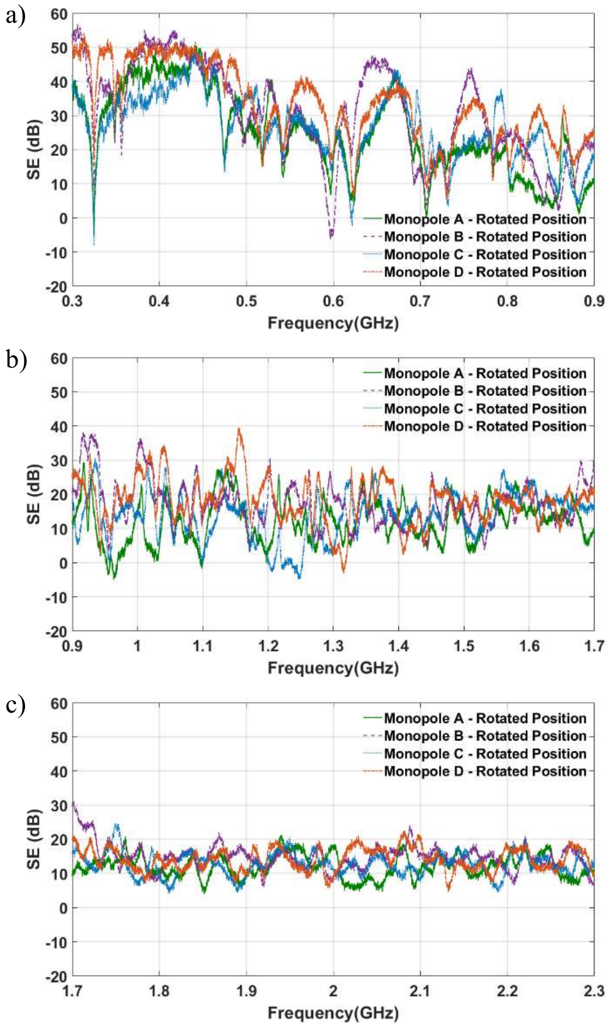

Fig. 9. Averaged SE calculated using the monopole antennas on the Antenna TL ReCo 180 degrees rotated, a) resonant region, b) transition region, and c) reverberant region.

To measure the field in the gap between the two of the TL ReCos (between the contents), the Antenna TL ReCo was rotated by 180° so that the monopoles faced the space between the stacked TL ReCos (the fourth and fifth TL ReCo). As shown in Fig. 9, the cavity between the fourth and fifth TL ReCos exhibits the same averaged SE behavior, displaying resonant, transition, and reverberant frequency regions.

Comparing Fig. 8 and Fig. 9, it can be observed that in the resonant range, rotating the Antenna TL ReCo results in the observation of more resonances as a result of the change in position of the monopoles. The spacing between the TL ReCos and their placement affects the field distribution, resonance characteristics, and, consequently, the shielding behavior of the cavity.

Figure 10 depicts the total standard deviation of the SE for all monopole antennas placed at eleven different positions within the enclosure, considering one hundred stirrer positions in the RC. The figure confirms that as frequency increases, the standard deviation decreases, indicating reduced variability in the averaged SE.

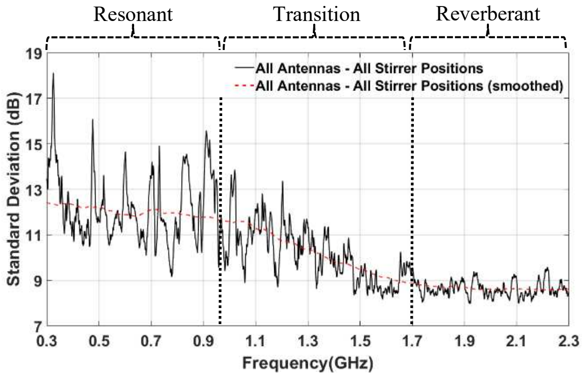

Fig. 10. The standard deviation of SE for all the eleven antennas considering all the hundred stirrer positions(black line), and smoothed line (red dashed line) to represent the resonant, transition, and reverberant regions.

The red line in Fig. 10 represents a smoothed behavior (moving average with 500MHz bandwidth), illustrating the overall transition more clearly by reducing fluctuations. Notably, in the resonant and reverberant regions, the red smoothed line remains relatively constant, whereas in the transition region, it exhibits a gradual decline, bridging the behavior between the two regions. Furthermore, the peaks in the standard deviation observed in the resonant region of Fig. 10 correspond to the minima of the averaged SE in the resonant region of Figs. 7 to 9.

The statistical distribution of measured SE for eleven different antenna positions within the enclosure at six arbitrary frequency points, two from each frequency region, is presented in Fig. 11. Within each region, the frequency points are chosen near local maxima and minima of standard deviation (Fig. 10). As shown in Fig. 11a, in the resonant region, the SE exhibits a broad distribution with relatively high standard deviations, further indicating significant SE variation across antenna positions. In the transition region (Fig. 11b), the standard deviation decreases compared to the resonant region, reflecting a shift toward a more stable SE distribution. Finally, in the reverberant region (Fig. 11c), the measured SE distribution becomes more uniform, exhibiting characteristics of a lognormal distribution of reverberant environment.

From these observations, it is evident that each set of antennas, whether mounted on the walls or the Antenna TL ReCo, produces consistent trends. Across all cases, the enclosure exhibits higher maxima and lower minima in terms of averaged SE at lower frequencies, with sharper resonances in the resonant range. Moreover, monopoles on the Antenna TL ReCo (within the center of the enclosure volume) frequently display the highest averaged SE maxima, whereas monopoles on the walls show the lowest averaged SE minima.

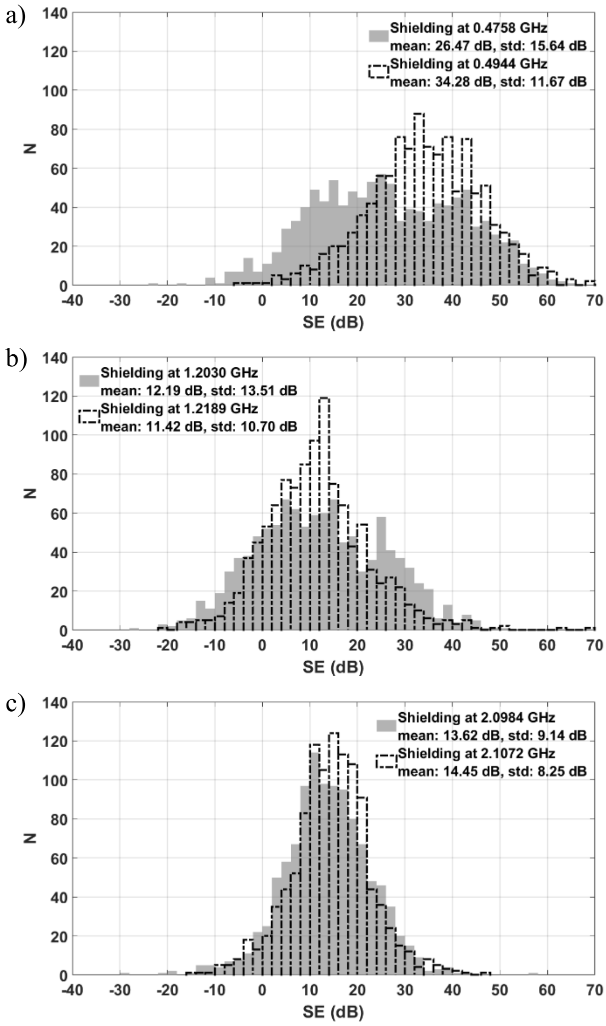

Fig. 11. Checking the distribution of measured SE for all eleven antenna positions at six different frequency points in three different frequency regions, a) resonant, b) transition, and c) reverberant.

The number and value of the averaged SE minima observed in the resonant range varies between the different monopole positions with no monopole showing the complete set of averaged SE minima. The higher averaged SE trend at lower frequencies is due to the enclosure aperture being electrically smaller at the lower frequencies.

As the frequency increases through the transition region into the reverberant region, the averaged SE values decrease, transitioning from high variability to more stable and less variable results.

These findings show the impact of frequency and antenna placement on SE behavior, with more predictable and uniform performance emerging in the reverberant range.

V. Conclusion

This study explores the shielding behavior of the enclosure across the reverberant, transition, and resonant frequency regions, with a specific focus on the existence of a transition region. Experimental results demonstrate that while enclosures exhibit stable shielding behavior in the reverberant range, significant variability emerges in the transition region before settling into discrete resonant modes at lower frequencies. Moreover, the measurements confirm that the SE of an enclosure is highly dependent on internal contents, antenna placement, and frequency, with the transition region acting as a critical boundary where field distributions change.

These findings emphasize the need for considering the transition region in SE evaluations, as conventional reverberant or resonant models alone may not fully explain enclosure performance in practical scenarios. Future work may further investigate predictive modeling approaches to better characterize SE behavior in the transition and resonant range, aiding the development of improved shielding strategies for electronic enclosures.

References

[1] A. Ghaffarlouy Raef, A. C. Marvin, S. J. Bale, M. P. Robinson, and J. F. Dawson, “Enhanced Prediction and Measurement of the Shielding Effectiveness of Reverberant Equipment Enclosures,” in 2024 International Symposium on Electromagnetic Compatibility – EMC Europe, Sep. 2024, pp. 595–600. doi: 10.1109/EMCEurope59828.2024.10722550.

[2] A. C. Marvin, S. L. Parker, J. F. Dawson, and M. P. Robinson, “Measurements and Power Balance Calculations of the Shielding Effectiveness of Partitioned Equipment Enclosures,” in 2019 International Symposium on Electromagnetic Compatibility - EMC EUROPE, Barcelona, Spain: IEEE, Sep. 2019, pp. 158–162. doi: 10.1109/EMCEurope.2019.8872077.

[3] D. Fedeli, G. Gradoni, V. M. Primiani, and F. Moglie, “Accurate Analysis of Reverberation Field Penetration Into an Equipment-Level Enclosure,” IEEE Trans. Electromagn. Compat., vol. 51, no. 2, pp. 170–180, May 2009, doi: 10.1109/TEMC.2009.2013456.

[4] “IEEE Standard Method for Measuring the Shielding Effectiveness of Enclosures and Boxes Having all Dimensions between 0.1 m and 2 m,” IEEE. doi: 10.1109/IEEESTD.2014.6712029.

[5] C. L. Holloway et al., “Use of Reverberation Chambers to Determine the Shielding Effectiveness of Physically Small, Electrically Large Enclosures and Cavities,” IEEE Trans. Electromagn. Compat., vol. 50, no. 4, pp. 770–782, Nov. 2008, doi: 10.1109/TEMC.2008.2004580.

[6] S. L. Parker et al., “Predicting shielding effectiveness of populated enclosures using absorption cross section of PCBs,” in 2016 International Symposium on Electromagnetic Compatibility - EMC EUROPE, Wroclaw, Poland: IEEE, Sep. 2016, pp. 324–328. doi: 10.1109/EMCEurope.2016.7739305.

[7] J. F. Dawson, A. C. Marvin, M. P. Robinson, and I. D. Flintoft, “On the Meaning of Enclosure Shielding Effectiveness,” in 2018 International Symposium on Electromagnetic Compatibility (EMC EUROPE), Amsterdam: IEEE, Aug. 2018, pp. 746–751. doi: 10.1109/EMCEurope.2018.8485121.

[8] I. D. Flintoft et al., “Representative Contents Design for Shielding Enclosure Qualification From 2 to 20 GHz,” IEEE Trans. Electromagn. Compat., vol. 60, no. 1, pp. 173–181, Feb. 2018, doi: 10.1109/TEMC.2017.2702595.